

Multi-criteria Design Optimization of Parallel Robots

Ramazan Unal
Mechatronics Program
Sabancı University
İstanbul, Turkey
ramazanunal@su.sabanciuniv.edu

Gullu Kiziltas
Mechatronics Program
Sabancı University
İstanbul, Turkey
gkiziltas@sabanciuniv.edu

Volkan Patoglu
Mechatronics Program
Sabancı University
İstanbul, Turkey
vpatoglu@sabanciuniv.edu

Abstract—This paper presents a framework for multi-criteria design optimization of parallel mechanisms. Pareto methods characterizing the trade-off between multiple design criteria are advocated for multi-criteria optimization over widely used scalarization approaches and Normal Boundary Intersection method is applied to efficiently obtain the Pareto-front hyper-surface. The proposed framework is compared against sequential optimization and weighted sum approaches. Dimensional synthesis of a sample parallel mechanism (five-bar mechanism) is demonstrated through estimation of the relative weights of performance indices that are implicit in the Pareto plot. The framework is computational efficient, applicable to any set of performance indices, and extendable to include any number of design criteria that is required by the application.

Index Terms—Multi-criteria design optimization, dimensional synthesis of parallel mechanisms, optimal design of parallel robots.

I. INTRODUCTION

Robotic manipulators with parallel kinematic chains are becoming increasingly common due to the inherent advantages they offer with respect to their serial counterparts. Parallel mechanisms possess compact designs with high stiffness and have low effective inertia since their actuators can be grounded in many cases. In terms of dynamic performance, high position and force bandwidths are achievable with parallel mechanisms thanks to their light but stiff structure. Besides, parallel mechanisms do not superimpose position errors at joints, hence can achieve high precision.

Since the performance of parallel mechanisms is highly sensitive to their dimensions, design optimization studies are absolutely necessary for these types of mechanisms [1]. Design optimization studies of such mechanisms with closed kinematic chains are significantly more challenging than serial ones. Parallel mechanisms have smaller workspace with possible singularities within the workspace and their analysis is considerably harder than the analysis of mechanisms with serial kinematic chains. Due to the additional complexities involved, the dimensional synthesis of parallel mechanisms is still an active area of research.

While performing dimensional synthesis of parallel mechanisms, various performance criteria such as kinematic and dynamic isotropy, stiffness, sensitivity, and transmission capability have to be considered *simultaneously*. The performance with respect to many of these criteria cannot be improved without deteriorating others; hence, design trade-offs are inevitable.

Determination of optimal dimensions with respect to many design criteria is a difficult problem and should be handled with multi-objective optimization methods so that trade-offs can be assigned in a systematic manner.

There exists several studies in literature in which multiple competing design criteria have been considered for design of parallel robots. The studies that can be categorized under *scalarization methods* address the multi-criteria optimization problem in an indirect manner, by first transforming it into a (or a series of) single objective (scalar) problem(s). Among these approaches, Hayward *et al.* define the relationship between multiple criteria and utilize sensitivities of these criteria to conduct a hierarchical optimization study [2]. Multiple objectives are considered sequentially in [3]–[6] by searching for parameter sets resulting in near optimal kinematic performance and then selecting the design exhibiting the best dynamic performance from this reduced parameter space. Task-priority [7], probabilistic weighting [8], composite index [9], and tabular methods [10] are among the other scalarization approaches that consider multiple criteria. Scalarization methods possess the inherent disadvantage of their aggregate objective functions requiring preferences or weights to be determined *a priori*, *ie.* before the results of the optimization process are actually known [11]. Since assigning proper weights or prioritizing different criteria is a problem dependent, non-trivial task, these techniques fall short of providing a general framework to the design of the parallel mechanisms.

Pareto methods, on the other hand, incorporate all performance criteria within the optimization process and address them simultaneously to find a set of non-dominated designs in the objective space. Once such a hyper-surface resolving the design trade-offs is obtained, an appropriate design on this hyper-surface can be selected taking into account other design requirements of the particular application in consideration. Pareto methods allow the designer to make an informed decision by studying a wide range of options, since they contain solutions that are optimum from an *overall* standpoint; unlike scalarization techniques that may ignore this trade-off viewpoint. Thanks to this feature, Pareto methods are better suited as a general solution framework for design optimization of parallel mechanisms, since they provide a better understanding of optimization problem allowing all the consequences of a decision with respect to all the objectives be explored.

Due to its transparent interpretation even for non-expert users, the most commonly used technique for generating points on the Pareto-front hyper-surface is to solve for optimal solutions of (convex) weighted sums of several objective functions for various different settings of weights [12], [13]. This traditional approach is an extension of the scalarization approaches and suffers from two major drawbacks: Weighted sum approach does not guarantee a uniform spread of Pareto points for an even spread of weights, and this approach cannot solve for points on the non-convex portions of the Pareto-front hyper-surface [14]. Without prior knowledge of the shape of the Pareto-front hyper-surface, it is not possible to estimate values of weights that map out a uniform spread of points on the Pareto-front hyper-surface, while increasing the number of weights does not result in points on the non-convex portions of the Pareto set. Therefore, ill-behaved nature of the weighted sum approach frequently results in under-represented regions of the Pareto-front hyper-surface and cause selection of an inferior design solution by failing to map important non-dominated ones.

Other methods exist in literature that directly attack the problem to solve for the Pareto set. As regards to employing these Pareto methods for design of parallel mechanisms, Krefft *et al.* recently applied a modified genetic algorithm (GA) to a problem with multiple objective functions and solved for the Pareto-front hyper-surface [4], [15]. Similarly in [16], GA is applied to multi-criteria optimization of a 2-DoF parallel robot. Despite their inherent advantage of resulting in multiple non-dominated design solutions within a single optimization search, GA approaches suffer from several disadvantages. Specifically, the convergence performance of GA is highly dependent on user-specified parameters such as sharing factor, and the results are very sensitive to these user-specified parameters. Moreover, GA methods demand inferior computational cost with increasing number of objective functions, hence cannot be easily adopted or scaled for use of more than two objective functions [17]. More importantly, GA might prematurely converge to sub-optimal solutions [18]. Finally, use of GAs to obtain Pareto front hyper-surface has the disadvantages of large computational expense as well as a tendency for clumping of solutions in objective space resulting in under-represented regions of the Pareto-front [11].

Finally, in [19] authors proposed a multi-objective design framework for optimization of parallel mechanisms based on Normal Boundary Intersection (NBI) method [20]. In [21] the proposed framework is applied to design of a 3RPS-R type robot for dual purpose application. The proposed framework is computationally efficient, applicable to any set of performance indices, and extendable to include any number of design criteria that is required by the application.

In this paper, the framework introduced in [19] is further studied and extended results are presented. Global kinematic and dynamic performance of parallel mechanisms over a pre-defined singularity free workspace are maximized simultaneously and the Pareto-front curve for these two criteria is obtained. The results are compared against sequential opti-

mization and weighted sum approaches. To facilitate the determination of the “best” solution of the Pareto set, estimation of the relative weights of performance indices that are implicit in the Pareto plot is demonstrated.

The paper is organized as follows: Section 2 introduces the sample mechanism used for the analysis, a 2-DoF parallel five-bar linkage. Section 3 introduces the performance indices used in this study and formulates the multi-criteria optimization problem. Section 4 explains the optimization methods used to address the multi-criteria optimization problem and is followed by results and their discussion in Section 5. Section 6 presents conclusions and future work.

II. FIVE-BAR LINKAGE

The optimization framework presented in this paper is applied to a 2-DoF five-bar parallel mechanism due to its sufficient richness with relative simplicity allowing better interpretation of the optimization problem at hand. Moreover, scalarization/aggregate methods have been applied to the multi-criteria optimization of this mechanism in the literature, rendering comparisons of different approaches possible. The methods discussed in this paper constitute a general framework for design optimization of parallel mechanisms and is by no means limited to the sample mechanism studied.

A five-bar mechanism can be characterized by lengths l_0 , l_1 , l_2 , l_3 and l_4 of its five links and three variables r , γ and ν defining the position and orientation of its workspace as shown in Figure 1. To quantify the orientation of each link, joint angles q_i ($i = 1..4$) measured from the x -axis are introduced. A five-bar mechanism with symmetric link lengths ($l_1 = l_4$, $l_2 = l_3$) and a symmetric workspace that is located parallel to the x and y -axes of the global coordinate system ($\gamma = \pi/2$, $\nu = \pi/2$) is selected in this study. Moreover, out of four possible assembly configurations, only the elbow-out posture, as depicted in Figure 1, is studied. Optimality of the above listed decisions in terms of both kinematic and dynamic performance have already been shown in the literature [6].

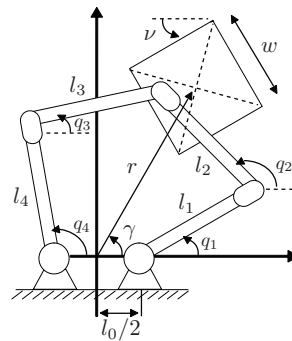


Fig. 1. Five-bar mechanism in the elbow-out posture

Assuming that the dimension of the symmetric workspace w is pre-determined, the optimization problem can be formulated using four design variables: l_0 , l_1 , l_2 and r . Table I presents the design variables α and design parameters β (parameters that do not change during the design process) for the symmetric five-bar mechanism.

TABLE I
DESIGN VARIABLES α AND PARAMETERS β

	Symbol	Definition	Unit
α_1	l_0	Distance between actuated joints	mm
α_2	l_1, l_4	Length of actuated links	mm
α_3	l_2, l_3	Length of free links	mm
α_4	r	Workspace center position	mm
β_1	$w = 100$	Workspace side length	mm
β_2	$\gamma = 90^\circ$	Angle between r and x -axis	$^\circ$
β_3	$\nu = 90^\circ$	Angle between W and y -axis	$^\circ$

III. OPTIMIZATION PROBLEM

Two objective functions characterizing the kinematic and dynamic performances of the mechanism are considered in this paper. To quantify the kinematic/dynamic performance of the parallel mechanism global isotropy index (\mathcal{GII}) and global dynamic index (\mathcal{GDI}) [6], are chosen. Both of these indices are conservative workspace inclusive worst-case performance measures that are intolerant of poor performance over the entire workspace. An optimal \mathcal{GII} results in a uniform kinematic Jacobian matrix, while optimizing \mathcal{GDI} minimizes the effective mass matrix of the system. Since the stiffness of the system is dominated by the compliance of the transmission and actuators, a Jacobian matrix with high isotropy not only results in the uniform kinematic behavior but also maximizes the stiffness of the device.

The objective of optimization is to maximize the worst kinematic isotropy of the mechanism (\mathcal{GII}) while simultaneously minimizing the effective mass (max singular value of the effective mass matrix or \mathcal{GDI}). The negative null form of the multi-objective optimization problem can be stated as

$$\begin{aligned} \max \quad & \mathbf{F}(\alpha, \beta, \gamma) \\ \mathbf{G}(\alpha, \beta) \leq & 0 \\ \alpha_a < \alpha < \alpha_u \end{aligned} \quad (1)$$

where \mathbf{F} represents the column matrix of objective functions that depend on the design variables α , parameters β , and workspace positions γ . Symbol \mathbf{G} represents the inequality constraint functions that also depend on design variables and parameters. Finally, α_l and α_u correspond to the lower and upper bounds of the design variables, respectively.

For the symmetric five-bar mechanism in elbow out posture, the column matrices \mathbf{F} and \mathbf{G} can be explicitly derived as

$$\mathbf{F} = \begin{bmatrix} \mathcal{GII} \\ \mathcal{GDI} \end{bmatrix}, \quad \mathbf{G} = \begin{bmatrix} (l_0/2 + w/2)^2 + (r + w/2)^2 - (l_1 + l_2)^2 \\ -q_2 \\ q_2 - q_1 \end{bmatrix}$$

In these expressions, the first element of the \mathbf{G} matrix constrains the design space to ensure a closed kinematic chain throughout the reachable workspace while last two elements stand for the elbow-out posture.

IV. METHODS

When the multi-criteria optimization problem is treated as multiple single objective problems where objective functions are handled independently, optimal solution for one criteria may result in an unacceptable design for the other. To achieve

a “best” solution with respect to multiple criteria, the trade-off between objectives needs to be negotiated. Scalarization approaches assumes apriori knowledge of this trade-off and converts the multi-criteria problem into a single objective one by assigning proper weights or priorities to each performance index. On the other hand, Pareto methods do not require any apriori knowledge about the design trade-offs and solve for the locus of all dominant solutions with respect to multiple objective functions, constituting the so-called the Pareto-front hyper-surface. Hence, designers can make a more realistic choice between multiple “best” solutions and avoid the challenge of synthetically ranking their preferences.

There exists several methods to obtain the Pareto-front hyper-surface, among which Normal Boundary Intersection (NBI) method is one of the most featured. As the Pareto-front hyper-surface is a geometric entity in the objective space forming the boundary of feasible region, NBI approach attacks the *geometric problem* directly by solving for single-objective constrained subproblems to obtain uniformly distributed points on the hyper-surface. NBI solves for subproblems which only depend on the defined optimization model, that is, chosen objective functions and design constraints since these equations map the feasible design space onto the attainable objective space. NBI obtains the Pareto-front with reducing the problem to many single-objective constrained geometric optimization subproblems. Number of subproblems can be adjusted by defining resolution of the grid that maps to the number of points on the Pareto-front hyper-surface. As the number of points increases, the computational time increases linearly, but since the method assumes spatial coherence and uses solution of a subproblem to initialize the next subproblem, convergence time for each subproblem may decrease resulting in further computational efficiency.

For a Pareto-front generation method can be classified as an effective one, the following criteria are to be satisfied [22]: minimum distance of the Pareto-front hyper-surface produced by the algorithm should be low with respect to the true Pareto-front hyper-surface and the maximum spread of solutions as well as maximum number of elements on the Pareto optimal set should be high.

NBI method results in exceptionally uniform distributed points on the Pareto-front hyper-surface without requiring any tuning of the core algorithm. Moreover, once shadow points are obtained, NBI solves for the geometric problem directly utilizing a fast converging gradient-based method, evading the computationally demanding aggregate optimization problems required in for most of the scalarization methods. Therefore, NBI method promises to be much faster and efficient than other methods to obtain a well represented Pareto-front hyper-surface including aggregate methods such as weighted sums and evolutionary optimization approaches such as GAs.

NBI method can solve for points on the non-convex regions of Pareto-front hyper-surfaces, a feature that is missing from the weighted sum methods. Existence of such non-convex Pareto sets for parallel mechanism is demonstrated in [21]. Compared to weighted sum techniques, NBI achieves higher

solution efficiency as it does not suffer from clumping of solution in the objective space. NBI is also advantageous over other methods as it trivially extends to handle any number of objective functions. Compared to Multi-Objective Genetic Algorithm (MOGA) [23] that requires problem dependent fitness and search related tuning and several steps to reach convergence, a standard NBI approach can map the Pareto-front hyper-surface with higher accuracy and uniformity, while also inheriting the efficiency of gradient-based methods.

Resulting in a uniform spread of points on the Pareto-front, NBI method provides sufficient information about the nature of trade-off between the objective functions in question. Once a such Pareto set is found, the next challenge is to determine the “best” solution out of this set. At this point, the relative weights that are implicit in the Pareto plot may help the designer. For the convex portions of the Pareto-front curve, there exists an explicit relationship between the slope of the Pareto curve at a Pareto point and the weighting coefficient λ [12], [14]. The weights possess an intuitive meaning and reflect the relative importance (preference) among the objective functions under consideration. If the Pareto set is representatively populated, a sufficiently high order polynomial curve fit can be performed in order to approximate the Pareto set. The polynomial fit to the Pareto set needs to be sufficiently high order to accurately represent the shape of the Pareto set. Once such a curve fit is obtained, the weight of every point on the convex parts of the curve can be estimated and these weights serve as helpful guides while negotiating the decision trade-offs within the Pareto set. The designer can choose from this set of solutions according to the relative satisfaction and preference of each objective.

Relying on gradient techniques, NBI assumes sufficient smoothness of the geometric problem at hand, but it has also been demonstrated that the method performs remarkably well even for non-smooth geometries [24]. In the presence of non-continuous regions, multiple initializations of the NBI method may be required for efficiently generating the Pareto-front hyper-surface. For the case of strongly discontinuous geometries, hybridization with MOGA-II to supply feasible initialization points at each continuous sub-region can be employed, as proposed in [24]. It is noted that since NBI relies on equality constraints, it is possible for NBI not to find a solution on the true Pareto-front hyper-surface, converging to a local optima. In such a case, post processing on the solutions of NBI subproblems can be employed to filter out undesired dominated solutions.

V. RESULTS AND DISCUSSION

To allow for comparisons of the proposed approach with other scalarization methods in the literature, sequential optimizations are implemented for the sample problem. In the first sequential approach (SA1), parameter sets resulting in the best \mathcal{GII} values for each discrete value of the parameter r are calculated. The change in \mathcal{GII} values and the link lengths are plotted in Figure 2 with respect to the independent parameter r . In this plot, one can observe that \mathcal{GII} value

increases monotonically with increasing r until the link length l_1 reaches its allowable upper limit (300mm) while link lengths l_0 and l_2 also increase with increasing r until l_2 reaches its allowable upper limit (300mm). Once l_2 reaches its upper limit, monotonic decrease in l_0 values can be observed until l_1 reaches its upper limit.

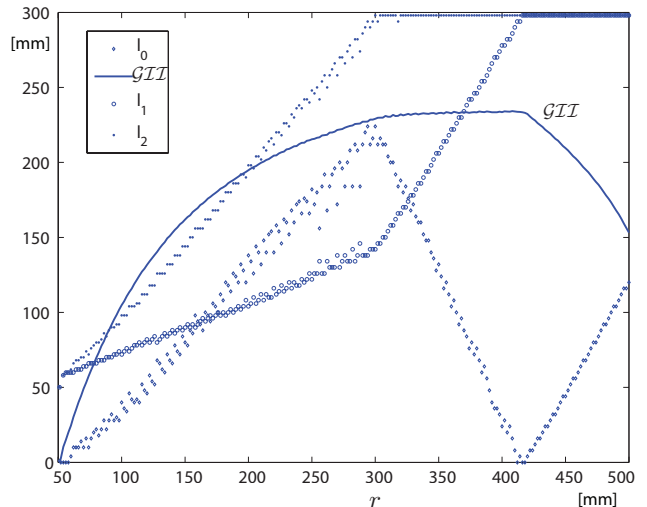


Fig. 2. Parameter sets with best \mathcal{GII} values for each discrete value of r .

Similarly for the second sequential approach (SA2), parameter sets resulting in the best \mathcal{GDI} values for each discrete value of the parameter r are calculated. The change in \mathcal{GDI} values and the link lengths are plotted in Figure 3 with respect to the independent parameter r . In this plot, one can observe that \mathcal{GDI} value increases for a while as the link lengths increase and after attaining its maximum value \mathcal{GDI} decreases monotonically. The increase in \mathcal{GDI} with the increasing link lengths take place due to the fact that \mathcal{GDI} is a measure of effective mass of the system, over which the kinematic Jacobian of the mechanism has high influence. At the low values of r , effects of kinematic Jacobian (hence the link lengths) dominate over the effects of link inertias and \mathcal{GDI} increases with the link lengths. At around $r = 80mm$, the effects of link inertias become more dominant and the expected trend of decrease of \mathcal{GDI} with increasing link lengths is observed. The optimal link lengths of the mechanism are highly affected by the upper limits. When link length l_2 reaches its allowable upper limit (300mm), l_1 starts a rapid increase until it encounters its own upper limit (300mm). Similarly, link lengths l_0 which stays very low up until l_2 reach its limit, starts increasing until l_1 reaches its upper limit, at which point l_0 experiences a sharp decrease.

Assigning r as the independent variable, the SA1 (SA2) uses the set of “optimal” solutions with respect to \mathcal{GII} (\mathcal{GDI}) as the feasible search domain to conduct another single criteria optimization, this time with respect to \mathcal{GDI} (\mathcal{GII}). In other words, the parameter set resulting in the best \mathcal{GDI} (\mathcal{GII}) value is selected from the Figure 2 (Figure 3). The results of the sequential optimization approaches are plotted in Figure 4

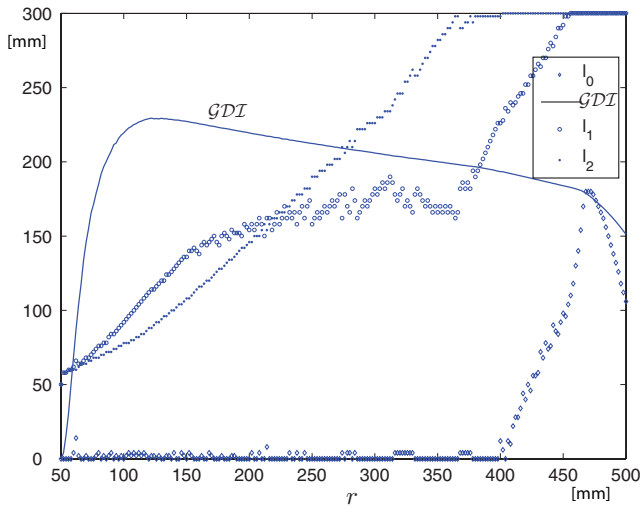


Fig. 3. Parameter sets with best GDI values for each discrete value of r .

with respect to a dense Pareto-curve obtained using the NBI approach. Inspecting the plot, one can conclude that the “best” solutions obtained using the sequential optimization approaches are both *dominated* – are points not lying on the Pareto front, meaning there exists solutions for which one can improve GII (GDI) while keeping GDI (GII) constant or vice versa. In fact, regrading to the solution of SA1 improvements up to 20% in the GII value and up to 3% in the GDI value are possible by choosing one of the designs that lies on the Pareto-front boundary found by the intersection of the Pareto curve and vertical and horizontal line, respectively, passing through that point. Similarly, improvements up to 20% in the GII value and up to 16% in the GDI value are possible for solution calculated by SA2.

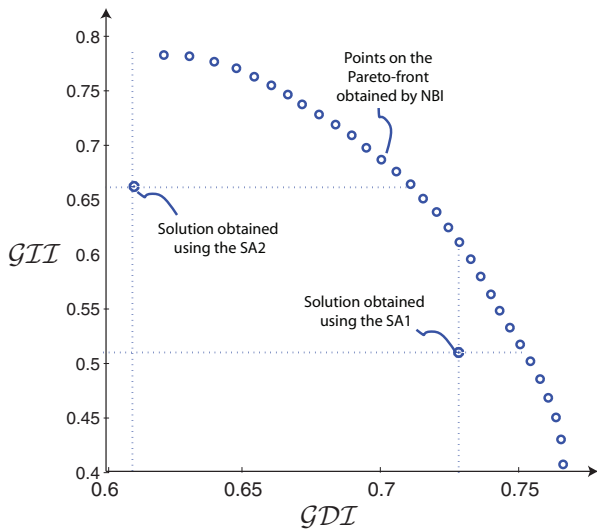


Fig. 4. Comparison of sequential approach with the Pareto-front curve.

To characterize the trade-off between the single objective solutions, Pareto-front curve for the bi-objective optimization problem is constructed in Figure 5 employing two different

techniques, namely NBI method and aggregated performance index method. For the NBI method, a grid size of ten points are selected. In Figure 5 the distribution of points on the Pareto-front curve is marked by dots. For the second method, an aggregated performance index (API) is defined as the weighted linear combination of GII and GDI . In particular, $API = \lambda GII + (1 - \lambda) GDI$, where $0 \leq \lambda \leq 1$ denotes the weighting factor. Ten aggregated optimization problems are solved for ten equally spaced weighting factors utilizing the modified culling algorithm with discretization step sizes of 5mm for the parameter space and 1mm for the workspace. Circles in the Figure 5 denote the distribution of aggregate solutions on the Pareto-front curve and are marked with their corresponding weighting factor.

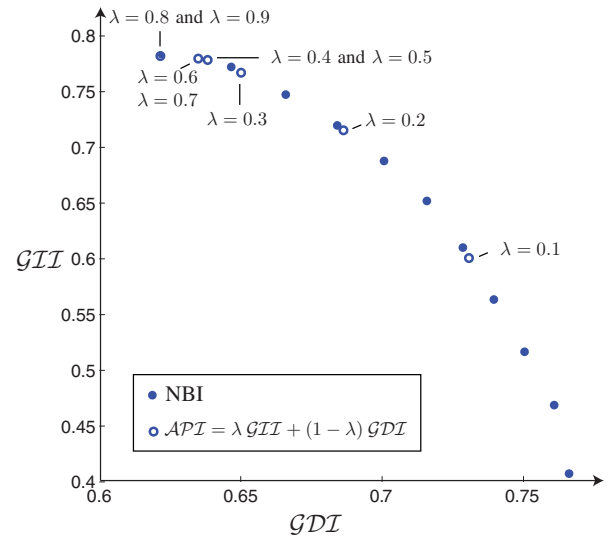


Fig. 5. Comparison of NBI and aggregated performance index methods. Symbol λ is the weighting factor.

As expected, NBI method generates a very uniform distribution of points on the Pareto-front curve while the solutions of the aggregate problem are clumped at certain locations of the curve. To obtain a uniform distribution using the aggregated index approach, proper weights should be assigned to ensure uniform distribution. However, the characteristics of the weight distribution is not known before the problem is solved. Moreover, since the aggregate performance index relies on the relatively costly culling algorithm to solve for each point on the Pareto-front curve, its accuracy is limited by the discretization step size chosen. In the Figure 5, the same solutions are obtained for different weighting factors, particularly for weighting factors $\lambda = 0.4$ to $\lambda = 0.5$, $\lambda = 0.6$ to $\lambda = 0.7$, and $\lambda = 0.8$ to $\lambda = 0.9$, respectively, due to the course discretization used. Unfortunately, solving for each aggregate performance index at each weighting is a computationally demanding task, limiting the density of feasible discretization. NBI method possesses an inherent advantage in terms of computational cost, as it attacks the direct geometric problem to obtain the Pareto-front curve and utilizes continuous, computationally efficient gradient methods for the solution.

In addition to the efficiency offered via the uniform distribution of solutions on the Pareto-front curve, NBI approach results in *orders of magnitude* improvement in the computation time, especially for the design problem at hand, as depicted in Figure 6. All of the simulations presented in Figure 6 are performed using a 32 bit Windows XP workstation that is equipped with a 3.40GHz Intel Xeon processor with 1MB L2 cache and 4GB DDR-2 400MHz SDRAM.

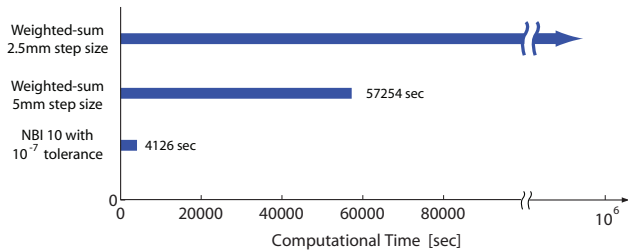


Fig. 6. Computational effort of NBI method and weighted sum method with respect to different discretizations.

As can be observed from Figure 6, the aggregate problem scales geometrically with the discretization step size, rendering an accurate solution of even ten points on the Pareto-curve almost impossible for the simple sample problem at hand. On the other hand, NBI method solves for points on the Pareto-front curve very effectively, in about 1/14 time of the weighted-sum approach with 5mm step size.

As emphasized earlier, any point on the Pareto-front curve is a non-dominated solution. Hence it is up to the designer to choose the “best” design for the application at hand, considering the characteristic of the trade-off mapped out by the Pareto-front boundary. This decision may be challenging since the relative weights are not transplant, but implicit in the Pareto plot. For the convex portions of the Pareto-front curve, it is always possible to estimate the relative weight λ of the objective functions since there exists an explicit relationship between the slope of the Pareto curve at a Pareto point and λ [14]. Reflecting the relative importance (preference) among the objective functions under consideration, weights help negotiating the decision trade-offs within the Pareto set. Note that, in contrast to the weighting sum approach, within the proposed framework the weights are obtained after the points representing the Pareto set are solved for. With such an approach the weights of points that are uniformly spread on the Pareto-front curve can trivially be constructed, a task that is not feasible with weighted sum approaches.

To estimate the weights of points on the Pareto set, a polynomial of 5th order is fitted with $R^2 = 0.9985$ on the points obtained using NBI method as shown in Figure 7. Given the slope (θ) of this curve at any point, relative weight λ of the objective functions can be estimated as $\lambda = 1/(1 - \theta)$.

The Pareto methods not only allow additional constraints be considered for the final decision but also let the designer adjust these constraints while simultaneously monitoring their effect on the set of non-dominated solutions. For the sample problem analyzed, a design is selected by imposing two additional

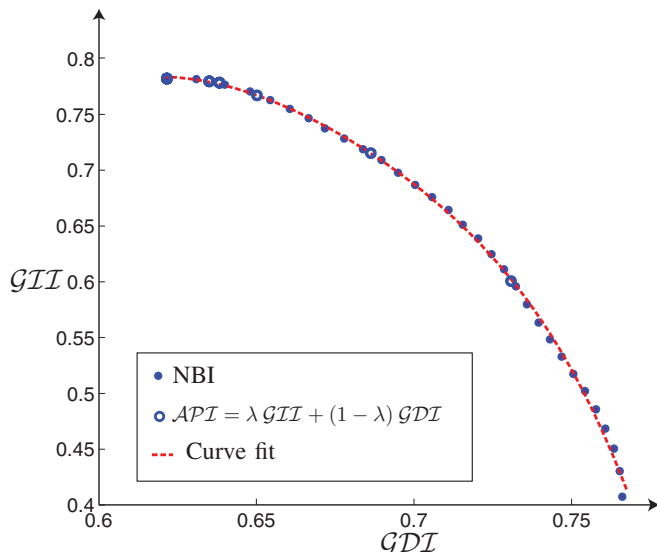


Fig. 7. Comparison of NBI and aggregated performance index methods. Symbol λ is the weighting factor.

physical constraints on the Pareto-front curve: a limit on the allowable workspace and a limit on the actuator size. Assuming that motors with 40mm diameter will be used as the actuators, a new lower limit can be imposed on the link lengths as $l_0 > 40\text{mm}$, rendering the last 11 points on the Pareto-front curve as infeasible designs. As for the second constraint, the footprint of the mechanism is to be restricted. The designer can impose constraints of different footprint areas to observe their effect on the non-dominated solution set. In Figure 8 infeasible solutions for footprint area of 400mm x 400mm are marked. Noticing that there are still many feasible solutions on the current Pareto-front curve, one can calculate the weights of the limit points of the feasible set using the curve fit. The limiting points have weights of $\lambda \approx 0.1$ and $\lambda \approx 0.2$, respectively. A final decision can be done considering the final use of the device in question. In this paper, the device is aimed to be used as a high fidelity haptic interface and more emphasis is given on the GDI value since this metric highly affects the closed loop control performance of the final design. Therefore, the point $\lambda \approx 0.1$, labeled as a star in Figure 8, is selected as the final design. The link lengths corresponding to this design choice are also represented in Figure 8.

VI. CONCLUSIONS AND FUTURE WORK

The framework introduced in [19] for optimization of mechanisms with closed kinematic chains, with respect to the multiple design criteria, is further studied and extended results are presented. Global kinematic and dynamic performance of parallel mechanisms over a pre-defined singularity free workspace are maximized simultaneously and the Pareto-front curve for these two criteria is obtained. The results are compared against sequential optimization and weighted sum approaches. The superiority of the design using Pareto methods is shown over prioritization approaches. To facilitate the determination of the “best” solution of the Pareto set,

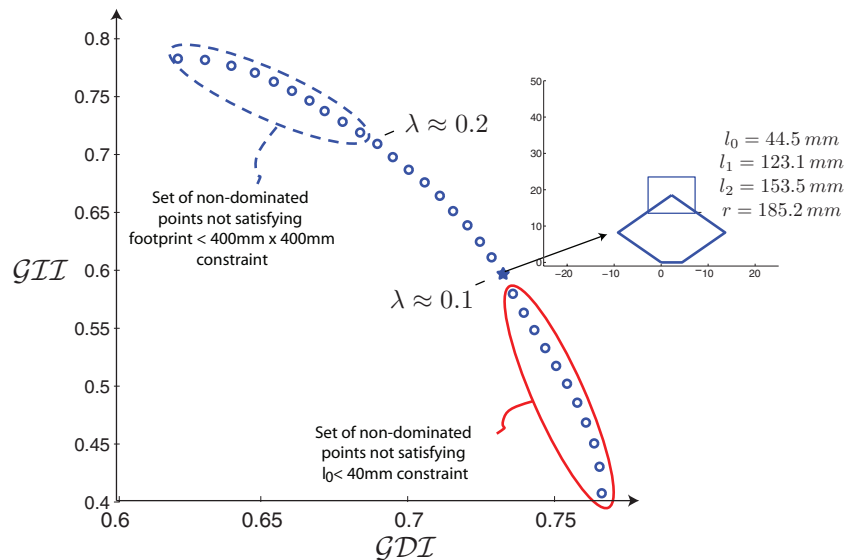


Fig. 8. Effects of additional constraints imposed on the problem and link lengths and weights corresponding to “best” designs.

estimation of the relative weights of performance indices that are implicit in the Pareto plot is demonstrated. Dimensional synthesis of a high performance parallel robot utilizing the fitted Pareto-front curve and extra constraints is demonstrated.

ACKNOWLEDGMENT

The authors gratefully acknowledge Aimin Zhou for his contributions during the implementation of NBI method and the support by TÜBİTAK with grant number 107M337.

REFERENCES

- [1] J. Merlet, *Parallel Robots*, 2nd ed. Springer, 2006.
- [2] V. Hayward, J. Choksi, G. Lanvin, and C. Ramstein, “Design and multi-objective optimization of a linkage for a haptic interface,” in *Advances in Robot Kinematics*, 1994, pp. 352–359.
- [3] G. Alici and B. Shirinzadeh, “Optimum synthesis of planar parallel manipulators based on kinematic isotropy and force balancing,” *Robotica*, vol. 22, no. 1, pp. 97–108, 2004.
- [4] M. Krefft, H. Kerle, and J. Hesselbach, “The assesment of parallel mechanisms – it is not only kinematics,” *Production Engineering*, vol. 12, no. 1, pp. 173–173, 2005.
- [5] A. Risoli, G. M. Prisco, F. Salsedo, and M. Bergamasco, “A two degrees-of-freedom planar haptic interface with high kinematic isotropy,” in *IEEE International Workshop on Robot and Human Interaction*, 1999, pp. 297–302.
- [6] L. Stocco, S. E. Salcudean, and F. Sassani, “Fast constrained global minimax optimization of robot parameters,” *Robotica*, vol. 16, no. 6, pp. 595–605, 1998.
- [7] W. Chen, Q. Zhang, Z. Zhao, and W. A. Gruver, “Optimizing multiple performance criteria in redundant manipulators by subtask-priority control,” in *IEEE International Conference on Systems, Man and Cybernetics*, 1995, pp. 2534–2539.
- [8] S. McGhee, T. F. Chan, R. V. Dubey, and R. L. Kress, “Probability-based weighting of performance criteria for a redundant manipulator,” in *IEEE International Conference on Robotics and Automation*, 1994, pp. 1887–1894.
- [9] J. H. Lee, K. S. Eom, B.-J. Yi, and I. H. Suh, “Design of a new 6-DoF parallel haptic device,” in *IEEE International Conference on Robotics and Automation*, vol. 1, 2001, pp. 886–891.
- [10] J. Yoon and J. Ryu, “Design, fabrication, and evaluation of a new haptic device using a parallel mechanism,” *IEEE Transactions on Mechatronics*.
- [11] O. L. de Weck, “Multiobjective optimization: History and promise,” in *China-Japan-Korea Joint Symposium on Optimization of Structural and Mechanical Systems*, ser. Invited Keynote Paper, 2004.
- [12] E. M. Kasprzak and K. E. Lewis, “An approach to facilitate decision tradeoffs in Pareto solution sets,” *Journal of Engineering Valuation and Cost Analysis*, vol. 3, no. 1, pp. 173–187, 2000.
- [13] I. Y. Kim and O. L. de Weck, “Adaptive weighted-sum method for bi-objective optimization: Pareto front generation,” *Journal Structural and Multidisciplinary Optimization*, vol. 29, pp. 149–158, 2005.
- [14] I. Das and J. Dennis, “A closer look at drawbacks of minimizing weighted sums of objectives for pareto set generation in multicriteria optimization problems,” *Journal Structural and Multidisciplinary Optimization*, vol. 14, no. 1, pp. 63–69, 1997.
- [15] M. Krefft and J. Hesselbach, “Elastodynamic optimization of parallel kinematics,” in *IEEE International Conference on Automation Science and Engineering*, 2005, pp. 357–362.
- [16] S.-D. Stan, V. Maties, and R. Balan, “Optimal design of 2 DoF parallel kinematics machines,” in *Applied Mathematics and Mechanics*, 2006, pp. 705–706.
- [17] C. A. Coello, “An updated survey of GA-based multiobjective optimization techniques,” *ACM Computing Surveys*, vol. 32, no. 2, pp. 109–143, 2000.
- [18] H. Ishibuchi and K. Narukawa, “Comparison of evolutionary multi-objective optimization with reference solution-based single-objective approach,” in *Genetic and Evolutionary Computation*, 2005, pp. 787–794.
- [19] R. Unal, G. Kiziltas, and V. Patoglu, “A multi-criteria design optimization framework for haptic interfaces,” in *IEEE International Symposium on Haptic Interfaces for Virtual Environments and Teleoperator Systems*, 2008, p. to appear.
- [20] I. Das and J. E. Dennis, “Normal-boundary intersection: A new method for generating the pareto surface in nonlinear multi-criteria optimization problems,” *SIAM Journal on Optimization*, vol. 8, no. 3, pp. 631–65, 1996.
- [21] R. Unal and V. Patoglu, “Optimal dimensional synthesis of a dual purpose haptic exoskeleton,” in *Springer in the Lecture Notes in Computer Science, EuroHaptics08*, submitted.
- [22] E. Zitzler, K. Deb, and L. Thiele, “Comparison of multiobjective evolutionary algorithms: Empirical results,” *Evolutionary Computation*, vol. 8, no. 2, pp. 149–172, 2000.
- [23] C. M. Fonseca and P. J. Fleming, “Genetic algorithms for multiobjective optimization: Formulation, discussion and generalization,” in *Multiobjective evolutionary algorithms: Empirical Genetic Algorithms*, 1993, pp. 416–423.
- [24] E. Rigoni and S. Poles, “NBI and MOGA-II, two complementary algorithms for multi-objective optimizations,” in *Practical Approaches to Multi-Objective Optimization*, 2005.